

Undissociated versus Dissociated Structures for Water Clusters and Ammonia–Water Clusters: $(\text{H}_2\text{O})_n$ and $\text{NH}_3(\text{H}_2\text{O})_{n-1}$ ($n = 5, 8, 9, 21$). Theoretical Study

S. Karthikeyan, N. Jiten Singh, and Kwang S. Kim*

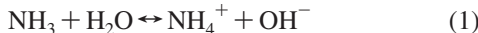
Center for Superfunctional Materials, Department of Chemistry, Pohang University of Science and Technology, San 31, Hyojadong, Namgu, Pohang 790-784, Korea

Received: February 26, 2008; Revised Manuscript Received: May 9, 2008

To understand the autoionization of pure water and the solvation of ammonia in water, we investigated the undissociated and dissociated (ion-pair) structures of $(\text{H}_2\text{O})_n$ and $\text{NH}_3(\text{H}_2\text{O})_{n-1}$ ($n = 5, 8, 9, 21$) using density functional theory (DFT) and second order Moller–Plesset perturbation theory (MP2). The stability, thermodynamic properties, and infrared spectra were also studied. The dissociated (ion-pair) form of the clusters tends to favor the solvent-separated ion-pair of $\text{H}_3\text{O}^+/\text{NH}_4^+$ and OH^- . As for the $\text{NH}_3(\text{H}_2\text{O})_{20}$ cluster, the undissociated structure has the internal conformation, in contrast to the surface conformation for the $(\text{H}_2\text{O})_{21}$ cluster, whereas the dissociated structure of $\text{NH}_3(\text{H}_2\text{O})_{20}$ has the surface conformation. As the cluster size of $(\text{H}_2\text{O})_n/\text{NH}_3(\text{H}_2\text{O})_{n-1}$ increases, the difference in standard free energy between undissociated and dissociated (ion-pair) clusters is asymptotically well corroborated with the experimental free energy change at infinite dilution of $\text{H}_3\text{O}^+/\text{NH}_4^+$ and OH^- . The predicted NH and OH stretching frequencies of the undissociated and dissociated (ion-pair) clusters are discussed.

I. Introduction

The solvation phenomena are ubiquitous in chemistry and biological sciences,¹ and the understanding of the phenomena is essential for molecular recognition, self-assembly, and design of ionophores and receptors for molecular sensors.² One of the important issues in the solvation process is to find how many solvent molecules are required to dissociate a solute molecule.^{3–5} Water autoionization is the most fundamental issue of solvation, and the solvation of ammonia in water is closely related to the water autoionization in view of its solvation mechanism. When an aqueous solution of a compound is basic, one water molecule donates its proton to a molecule of the basic compound, which results in the formation of cations and OH^- ions. A prototypical system for a weak base is the solution of ammonia in water, which shows the following equilibrium condition:



The experimental equilibrium constant for this reaction is 1.77×10^{-5} at room temperature (the standard free energy change ΔG_{298} is 6.48 kcal/mol),⁶ which is much greater than the autoionization constant of pure water (10^{-14}). Although the concentration of NH_4^+ and OH^- ions in aqueous ammonia is small (4.21×10^{-3} M), it is 4 orders greater in magnitude than the OH^- ion concentration in pure water.

The $\text{NH}_3(\text{H}_2\text{O})$ complex has been experimentally studied by microwave and far-infrared spectroscopy⁷ and by ab initio calculations.⁸ Donaldson⁹ studied the structure, thermodynamics, and kinetics of the formation of $\text{NH}_3(\text{H}_2\text{O})_{n=1,2}$ complexes, reporting the global minimum structure of these molecules. Lee et al. and Bacelo have shown that at least four water molecules are necessary to make the ion-pair cluster.¹⁰ The $\text{NH}_3(\text{H}_2\text{O})_4$ cluster can have a dissociated (ion-pair) structure $[\text{NH}_4^+ \cdots (\text{H}_2\text{O})_3 \cdots \text{OH}^-]$ as a local minimum where a proton

is transferred from a water molecule to the ammonia molecule. However, there is no detailed theoretical or experimental information about $\text{NH}_4^+ \cdots (\text{H}_2\text{O})_n \cdots \text{OH}^-$ for large n for which we here investigate the structures and dissociation energetics.

The structure, thermodynamic properties, and spectra of small water clusters have been a prime focus of experimental^{11,12} and theoretical investigations,^{13–22} due to their potential importance in understanding various phenomena such as ion solvation as well as solvent effects in biological and chemical systems.²³ It is a challenging task to study autoionization in water clusters because in the liquid state only a small amount of water (10^{-7} M) will be dissociated into H_3O^+ and OH^- ions at pH = 7.

In this study, we report the structure, stability, thermodynamic properties, and infrared (IR) spectra of the most stable undissociated and dissociated $(\text{H}_2\text{O})_n$ clusters and those of $\text{NH}_3(\text{H}_2\text{O})_{n-1}$ ($n = 5, 8, 9, 21$). These results are compared with the experimental water autoionization constant and acid–base equilibrium constant at 298 K. We also discuss differences between the $(\text{H}_2\text{O})_n$ clusters and $\text{NH}_3(\text{H}_2\text{O})_{n-1}$ clusters.

II. Computational Methods

To find the lowest energy structures,²⁴ we employed the basin-hopping global optimization with the density functional based tight-binding (DFTB) theory.²⁵ For the low lying energy structures, we carried out geometry optimization and total energy calculations using Becke's three parameters with Lee–Yang–Parr (B3LYP) functionals, Moller–Plesset second order perturbation theory (MP2), and resolution of the identity approximation (RI) MP2(RI-MP2).²⁶ All atoms were treated using the 6-311++G(d,p) basis set for B3LYP and the aug-cc-pVDZ basis set for MP2. The basis set superposition error (BSSE) corrections²⁷ were taken into account. The harmonic vibrational frequencies and the corresponding thermodynamic quantities were evaluated on the B3LYP/6-311++G (d,p) optimized geometries. These frequencies were used to obtain the zero point energies (ZPEs)

* To whom correspondence should be addressed. E-mail: kim@postech.ac.kr.

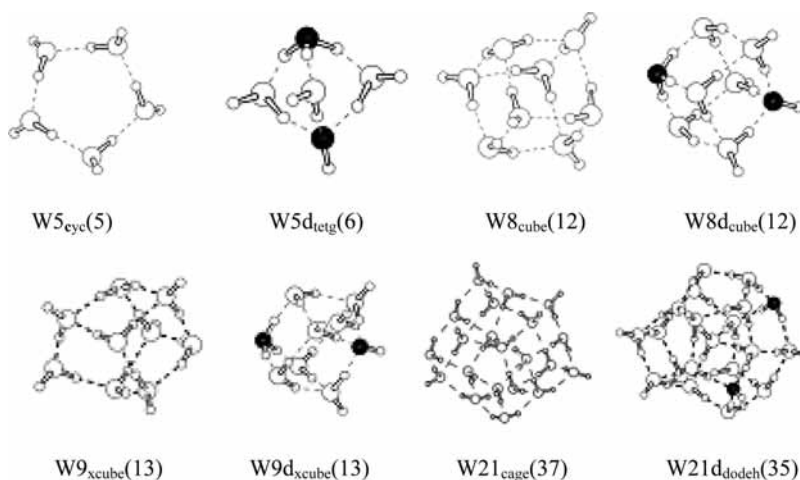


Figure 1. Lowest energy structures of undissociated and dissociated (ion-pair) water clusters $(\text{H}_2\text{O})_n$ ($n = 5, 8, 9, 21$). The number of hydrogen bonds is given in parentheses.

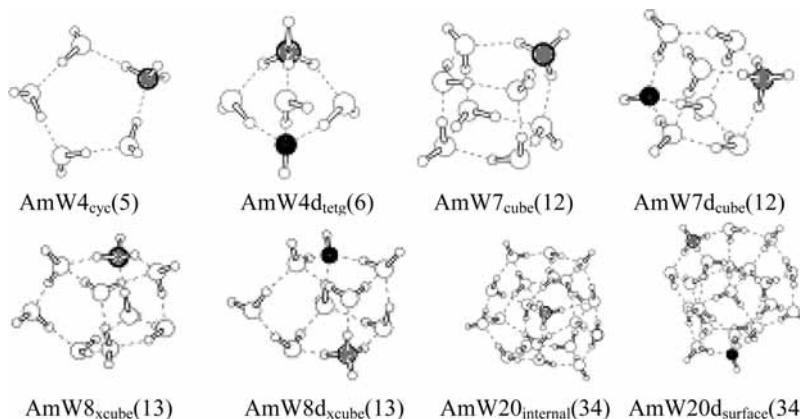


Figure 2. Lowest energy structures of undissociated and dissociated (ion-pair) ammonia–water clusters $\text{NH}_3(\text{H}_2\text{O})_{n-1}$ ($n = 5, 8, 9, 21$). The number of hydrogen bonds is in parentheses.

and thermal energies. The ZPE-corrected binding energies (ΔE_0), standard state enthalpy (ΔH_{298}), and free energies (ΔG_{298}) from the ZPE-uncorrected binding energies (ΔE_c) are reported. The B3LYP and MP2 calculations were performed with the GAUSSIAN 03 suite of programs,²⁸ and RI-MP2 calculations were performed with the TURBOMOLE suite.²⁹ All of the figures presented here were drawn using the POSMOL package.³⁰

III. Results and Discussion

We have investigated the undissociated and dissociated (ion-pair) structures of $(\text{H}_2\text{O})_n$ and $\text{NH}_3(\text{H}_2\text{O})_{n-1}$ ($n = 5, 8, 9, 21$) clusters. For the dissociated structures, the H_3O^+ and OH^- ions tend to form an ion-pair (either contact ion-pair or solvent-separated ion-pair). Thus, this dissociated case is closely related to the hydration of H_3O^+ and OH^- ions.^{31,32} There are many low energy structures for both undissociated and dissociated forms of water and ammonia–water clusters. The most stable structures are given in Figures 1 and 2. The relative energies of various structures of $(\text{H}_2\text{O})_n$ and $\text{NH}_3(\text{H}_2\text{O})_{n-1}$ are calculated at the B3LYP/6-31G* level of theory. The lowest energy undissociated and dissociated structures of the water clusters and ammonia–water clusters for each n are further investigated at the B3LYP/6-311++G** and MP2/aug-cc-pVQZ (or RIMP2/aug-cc-pVQZ) levels of theory. The results are given in Tables 1 and 2. The contribution of zero point energy (ZPE) corrections to the undissociated and dissociated (ion-pair) structures is found

to be almost same. Accurate evaluation of binding energies generally requires very large basis sets to minimize the errors in the interaction energies arising from both BSSE and basis set incompleteness error (BSIE) effects.³³ We have often found it useful to employ moderately sized basis sets for a large system with a 50% BSSE correction,^{18,33} thereby, the binding energy is between the BSSE-corrected and BSSE-uncorrected values as the lower and upper limits, respectively.

For the undissociated $(\text{H}_2\text{O})_5$ and $\text{NH}_3(\text{H}_2\text{O})_4$ clusters, the cyclic structure with five hydrogen bonds is the most stable, while in the dissociated (ion-pair) clusters the conformer with three tetragonal rings (tetg) is the most stable. Both undissociated and dissociated (ion-pair) $(\text{H}_2\text{O})_8$ and $\text{NH}_3(\text{H}_2\text{O})_7$ clusters have the cubic structure (cube) with 12 hydrogen bonds. Both undissociated and dissociated (ion-pair) $(\text{H}_2\text{O})_9$ and $\text{NH}_3(\text{H}_2\text{O})_8$ clusters show the extended cubic structures (xcube) with 13 hydrogen bonds.

For the undissociated $\text{NH}_3(\text{H}_2\text{O})_{20}$ cluster, the NH_3 has four well-balanced, tetrahedrally oriented hydrogen bonds inside the cage. Thus, we find from our calculations that the cluster with the NH_3 inside the cage (AmW20_{internal}) is more stable than the cluster with the NH_3 on the surface of the cage because of the presence of one additional hydrogen bond. However, for the undissociated $(\text{H}_2\text{O})_{21}$ cluster, we find that the cage type structure is 8.06 kcal/mol more stable than the internal type structure. It should be noted that the structure of the undissociated $\text{NH}_3(\text{H}_2\text{O})_{20}$ cluster is quite different from that of the

TABLE 1: Relative Energies and Thermodynamic Properties (kcal/mol) of the Lowest Energy Dissociated (Ion-Pair) Water Clusters with Respect to the Lowest Energy Undissociated Ones^a

B3LYP/6-311++G**(MP2/aug-cc-pVDZ)				
	$-\Delta E_c$	$-\Delta E_0$	$-\Delta H_{298}$	$-\Delta G_{298}$
W5d _{tetg}	21.69 ± 1.12 (22.13 ± 2.25)	20.73 (21.17)	19.02 (19.46)	23.89 (24.33)
W8d _{cube}	16.31 ± 1.21 (18.33 ± 2.09)	14.86 (16.91)	13.56 (15.58)	16.37 (18.39)
W9d _{xcube}	15.78 ± 1.13 (17.52 ± 2.07)	14.29 (16.03)	12.96 (14.71)	15.91 (17.66)
W21d _{dodeh}	10.07 ± 1.12 (11.27 ± 2.06)	9.14 (10.34)	7.77 (8.97)	10.18 (11.38)
$n = \infty$ [expt]				[8.40]

^a The zero point energy correction is made with the B3LYP/6-311++G** value. The MP2 binding energy for W21d_{dodeh} is calculated with the RI-MP2 method. The binding energy is given by the median value of ZPE-uncorrected and -corrected values, which are likely to be the upper and lower limit values, respectively. The value after “±” is the half of the BSSE.

TABLE 2: Relative Energies (kcal/mol) of the Lowest Energy Dissociated (Ion-Pair) Ammonia–water Cluster with Respect to the Lowest Energy Undissociated Ones^a

B3LYP/6-311++G**(MP2/aug-cc-pVDZ)				
	$-\Delta E_c$	$-\Delta E_0$	$-\Delta H_{298}$	$-\Delta G_{298}$
AmW4d _{tetg}	13.31 ± 0.80 (12.62 ± 1.75)	13.57 (12.87)	12.14 (11.44)	16.46 (15.76)
AmW7d _{cube}	7.66 ± 0.88 (8.91 ± 1.44)	7.66 (8.91)	6.47 (7.72)	9.21 (10.46)
AmW8d _{cube}	6.92 ± 0.80 (7.89 ± 1.39)	6.97 (7.94)	5.76 (6.73)	8.67 (9.64)
AmW20d _{surface}	4.86 ± 0.78 (6.05 ± 0.96)	4.90 (6.09)	3.61 (4.60)	6.81 (7.80)
$n = \infty$ [expt]				[6.48]

^a The zero point energy correction is made with the B3LYP/6-311++G** value. The MP2 binding energy for AmW20d_{dodeh} is calculated with the RI-MP2 method.

undissociated $(H_2O)_{21}$ cluster, whereas the structure of the dissociated (ion-pair) $NH_3(H_2O)_{20}$ cluster is similar to that of the dissociated (ion-pair) $(H_2O)_{21}$ cluster. Each hydrogen atom of the H_3O^+ ion involves a hydrogen bond as a strong hydrophilic site, whereas the oxygen atom of the H_3O^+ ion behaves as a hydrophobic site due to the three positively charged hydrogen atoms that hinder the close approach of other hydrogen atoms toward the oxygen center. The H_3O^+ ion tends to be on the surface of the cluster, and the three hydrogen atoms of the H_3O^+ ion are bonded by three ADD (in which A and D denote proton acceptor and donor, respectively) type water molecules. Thus, the H_3O^+ ion favors the trihydrogen-bonded structure. The dissociated (ion-pair) conformers of both water cluster (W21d_{dodeh}) and ammonia–water cluster (AmW20d_{surface}) show the surface structures of the cage form which maximize the polarization effect, where the letter “d” denotes the dissociated structure. For the undissociated $NH_3(H_2O)_{20}$ cluster, the internal type structure is more stable than the surface type structure. However, for the dissociated (ion-pair) $NH_3(H_2O)_{20}$ cluster, the surface type structure is much more stable than the internal type structure. For the dissociated (ion-pair) form of these clusters, the cation (H_3O^+ , NH_4^+) tends to be separated from the OH^- ion by more than one water molecule.

We investigate the relative change in free energy of undissociated and dissociated (ion-pair) forms of $(H_2O)_n$ and $NH_3(H_2O)_{n-1}$ ($n = 5, 8, 9, 21$), which are found to decrease with the increase in number of water molecules in ammonia–water clusters. In the case of $(H_2O)_{21}$, the dissociated (ion-pair) W21d_{dodeh} cluster is less stable than the undissociated W21_{cage} cluster by 11.27/10.34 kcal/mol in ZPE-uncorrected/corrected binding energy ($\Delta E_c/\Delta E_0$) and 11.38 kcal/mol in free binding energy ($-\Delta G_{298}$) at the RIMP2/aug-cc-pVDZ level. In the case of $NH_3(H_2O)_{20}$, the dissociated (ion-pair) AmW20d_{surface} cluster is less stable than the undissociated AmW20_{internal} cluster by 6.05/6.09 kcal/mol in $\Delta E_c/\Delta E_0$ and 7.80 kcal/mol in ΔG_{298} at the RIMP2/aug-cc-pVDZ level. Figure 3 shows the plot of ΔG_{298} with respect to $1/n$, where n is the number of water molecules in the cluster. The extrapolated values of the two

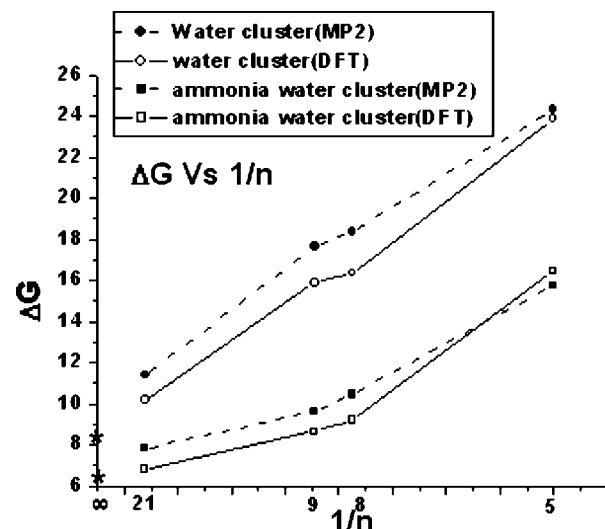


Figure 3. ΔG vs $1/n$ where n is the number of water molecules. The experimental free energy change at infinite dilution is denoted by an asterisk. (ΔG is in kcal/mol.)

curves to infinite dilution show good agreements with the corresponding experimental values.

The O–H and N–H stretching frequencies are widely used to identify their diverse H-bonded structures.³⁴ The scale factor 0.96 at the B3LYP level of theory was chosen from the comparison of the experimental and calculated average values of asymmetric and symmetric OH stretching frequencies of the water monomer.³⁵ Since the IR spectral information would be useful for the identification of hydrogen-bonding structures, the IR spectra of the most stable undissociated and dissociated (ion-pair) structures of $(H_2O)_{21}$ and $NH_3(H_2O)_{n=4,7,8,20}$ are given in Figure 4 and in the Supporting Information (Table S1). It is interesting to note that the dissociated (ion-pair) structures of $NH_3(H_2O)_{n=4,7,8,20}$ show peaks around $2200\text{--}2600\text{ cm}^{-1}$, while their undissociated structures show no peaks for $1800\text{--}2800\text{ cm}^{-1}$ except for $n = 20$ showing a peak at 2443 cm^{-1} , which reflects the internal structure.

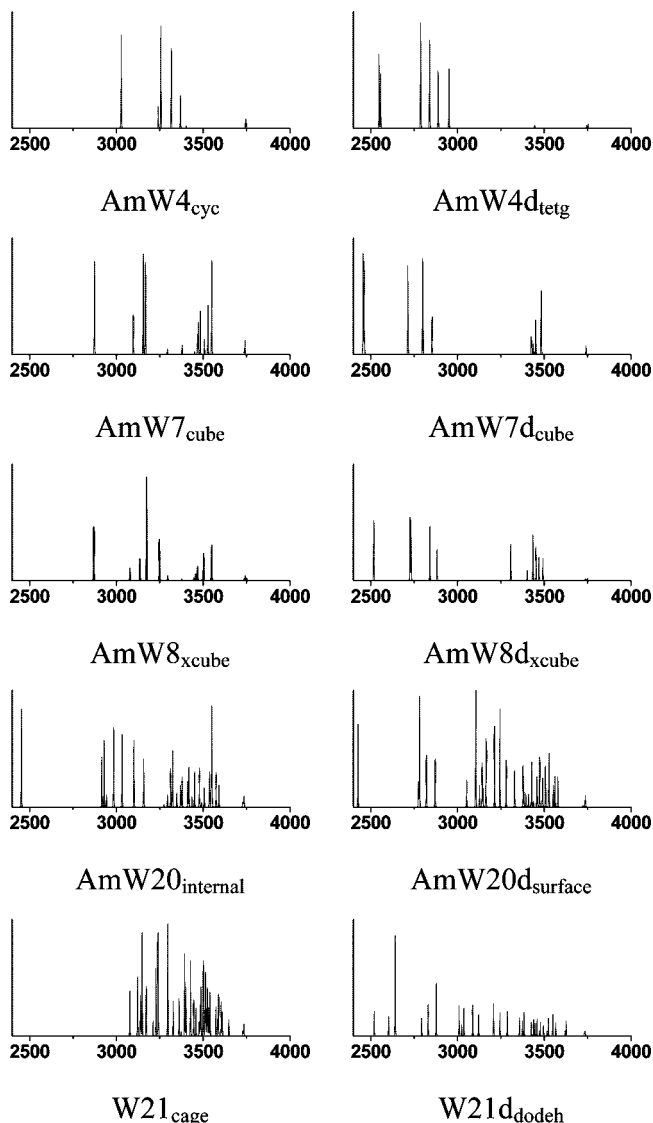


Figure 4. B3LYP/6-311++G** IR spectra for the N–H and O–H vibration frequencies of the undissociated and dissociated (ion-pair) $\text{NH}_3(\text{H}_2\text{O})_{n-1}$ ($n = 5, 8, 9, 21$) and $(\text{H}_2\text{O})_{n=21}$ (scale factor 0.96).

As for the free NH stretching frequencies, the undissociated $\text{NH}_3(\text{H}_2\text{O})_n$ for $n = 4, 7$, and 8 show the peaks at $3441, 3435$, and 3431 cm^{-1} , respectively, while the undissociated $\text{NH}_3(\text{H}_2\text{O})_{20}$ has no free NH-stretching frequency. The ion-pair ammonia–water clusters for $n = 4, 7, 8$, and 20 show peaks at $3430, 3422, 3421$, and 3408 cm^{-1} , respectively, which are slightly red-shifted compared with the undissociated cases. For the hydrogen-bonded NH stretching frequencies, the undissociated $\text{NH}_3(\text{H}_2\text{O})_n$ for $n = 4, 7, 8$, and 20 show the peaks at $(3227, 3389), (3280, 3365), (3282, 3362)$, and $(3261, 3362) \text{ cm}^{-1}$, respectively, while the dissociated (ion-pair) clusters for $n = 4, 7, 8$, and 20 show the peaks at $(2827, 2876, 2939), (2787, 2789, 2841), (2721, 2829, 2870)$, and $(2764, 2809, 2859, 3408) \text{ cm}^{-1}$, respectively. Thus, the hydrogen-bonded NH stretching frequencies substantially red-shift in the ion-pair structures. The NH stretching frequencies of undissociated and dissociated (ion-pair) ammonia–water clusters decrease with increasing number of water molecules in the cluster due to the polarization effect similar to what we observed in neutral water clusters.¹⁸

The stretching frequencies of free OH (AD: acceptor–donor) and hydrogen-bonded OH (AD) for the undissociated

$\text{NH}_3(\text{H}_2\text{O})_4$ appear at $(3728, 3729, 3731, 3733)$ and $(3015, 3243, 3302, 3355) \text{ cm}^{-1}$, respectively, while those of the dissociated $\text{NH}_3(\text{H}_2\text{O})_4$ appear at $(3729, 3737, 3738)$ and $(2538, 2547, 2776) \text{ cm}^{-1}$, respectively. The free OH (AAD: acceptor–acceptor–donor) stretching frequencies of the undissociated ammonia–water clusters for $n = 7, 8$, and 20 show peaks at $(3721, 3725), (3721, 3726–3728)$, and $(3711–3721) \text{ cm}^{-1}$, respectively, while those of the ion-pair ammonia–water cluster for $n = 7, 8$, and 20 show peaks at $(3724–3726), (3719–3726)$, and $(3708–3722) \text{ cm}^{-1}$, respectively. The hydrogen-bonded OH (ADD) stretching frequencies of the undissociated ammonia–water cluster for $n = 7, 8$, and 20 show peaks at $(3453–3534), (3442–3534)$, and $(3334–3576) \text{ cm}^{-1}$, respectively, while those of the ion-pair ammonia–water clusters for $n = 7, 8$, and 20 show peaks at $(3410–3468), (3387–3477)$, and $(3367–3563) \text{ cm}^{-1}$, respectively. The stretching frequencies of hydrogen-bonded OH (AAD) of the undissociated ammonia–water cluster for $n = 7, 8$, and 20 show peaks at $(2862, 3084, 3142, 3154), (2858, 3065, 3161, 3235)$, and $(2904–3310) \text{ cm}^{-1}$, respectively, while those of the ion-pair ammonia–water clusters for $n = 7, 8$, and 20 show peaks at $(2446, 2452, 2703), (2335, 2507, 2715)$, and $(2242, 2769, 3040, 3092, 3114, 3150) \text{ cm}^{-1}$, respectively. Thus, as the cluster dissociates into the ion-pair, the ADD-type OH frequencies red-shift slightly, while the AAD-type OH frequencies red-shift substantially.

The hydrogen-bonded OH (AADD: acceptor–acceptor–donor–donor) stretching frequencies of the undissociated and dissociated $\text{NH}_3(\text{H}_2\text{O})_{20}$ show peaks at $(2443, 3462, 3464, 3467, 3530, 3534, 3537, 3559)$ and $(2417, 3129, 3134, 3200, 3230, 3255, 3266, 3315, 3364, 3442) \text{ cm}^{-1}$, respectively. While their ranges decrease with increasing number of water molecules in both undissociated and ion-pair clusters, the hydrogen-bonded OH stretching frequencies of the dissociated clusters appear lower than those of the undissociated clusters.

The stretching frequencies of the OH^- ions of the ion-pair ammonia–water cluster for $n = 4, 7, 8$, and 20 show peaks at $3727, 3717, 3710$, and 3704 cm^{-1} , respectively. The stretching frequencies of OH^- ions decrease with increasing number of water molecules in the cluster due to the polarization effect.

For the undissociated $(\text{H}_2\text{O})_{21}$, the stretching frequencies appear at $3711–3719 \text{ cm}^{-1}$ for free OH (AAD) and appear in the range of $3065–3632 \text{ cm}^{-1}$ for the hydrogen-bonded OH (ADD, AAD, AADD, and AAAD). For the dissociated $(\text{H}_2\text{O})_{21}$, the stretching frequencies appear at $3715–3721 \text{ cm}^{-1}$ for free OH (AAD) and at $2509–3611 \text{ cm}^{-1}$ for hydrogen-bonded OH (ADD, AAD, and AADD).

In contrast to $\text{NH}_3(\text{H}_2\text{O})_{20}$, the undissociated $(\text{H}_2\text{O})_{21}$ cluster shows no peaks in the range of $1800–3000 \text{ cm}^{-1}$. However, the dissociated ion-pair $(\text{H}_2\text{O})_{21}$ cluster shows asymmetric and symmetric stretching frequencies of the H_3O^+ ion at 2592 and 2819 cm^{-1} , respectively. The stretching frequencies associated with dangling hydrogen atoms appear in the range of $3715–3721 \text{ cm}^{-1}$, and the stretching frequency of the OH^- ion appears at 3714 cm^{-1} .

IV. Concluding Remarks

Using the B3LYP and MP2 calculations, we have studied the structure, stability, thermodynamic properties, and IR spectra of both undissociated and ion-pair forms of water clusters $(\text{H}_2\text{O})_n$ and ammonia–water clusters $\text{NH}_3(\text{H}_2\text{O})_{n-1}$ ($n = 5, 8, 9, 21$). The dissociated (ion-pair) form of the clusters tends to favor the solvent-separated ion-pair of $\text{H}_3\text{O}^+/\text{NH}_4^+$ and OH^- . As for the structure, it is particularly interesting to note that, for the $\text{NH}_3(\text{H}_2\text{O})_{20}$ cluster, the undissociated cluster shows the

internal structure, while the dissociated (ion-pair) conformer shows the surface structure which maximizes the polarization effect. The undissociated $NH_3(H_2O)_{20}$ cluster is quite different in structure from that of the undissociated $(H_2O)_{21}$ cluster, whereas the ion-pair $NH_3(H_2O)_{20}$ cluster is similar in structure to the ion-pair $(H_2O)_{21}$ cluster. The free energy changes (ΔG_{298}) required for the dissociation are found to decrease with the increase in number of water molecules. These predicted asymptotic values of the free energy changes for the infinite number of water molecules are in good agreement with the experimental free energies at infinite dilution. The free energy changes required for the dissociation of water clusters are larger than those of ammonia–water clusters, possibly because water clusters are more polar than ammonia–water clusters. As the number of water molecules in the undissociated and dissociated (ion-pair) clusters increases, the increasing polarization tends to decrease the NH and OH stretching frequencies. The hydrogen-bonded OH stretching frequencies of the dissociated clusters appear lower than those of the undissociated clusters. As the cluster dissociates into the ion-pair, the hydrogen-bonded NH stretching frequencies red-shift substantially, and the ADD-type OH frequencies red-shift slightly, while the AAD-type OH frequencies red-shift substantially. In contrast to $NH_3(H_2O)_{20}$, the undissociated $(H_2O)_{21}$ cluster shows no peaks in the range of 1800–3000 cm^{-1} .

Acknowledgment. This work was supported by BK21 and KRF (KICOS).

Supporting Information Available: Calculated N–H and O–H stretching frequencies of the undissociated and dissociated (ion-pair) $NH_3(H_2O)_n$ ($n = 4, 7, 8, 20$) and $(H_2O)_{21}$. This material is available free of charge via the Internet at <http://pubs.acs.org>.

References and Notes

- (1) (a) Dogonadze, R. R.; Kalman, E.; Kornyshev, A. A.; Ulstrup, J. *Chemical Physics of Solvation: Solvation Phenomena in Specific Physical, Chemical and Biological Systems*; Elsevier: Amsterdam, 1988. (b) Singh, N. J.; Olleta, A. C.; Kumar, A.; Park, M.; Yi, H.-B.; Bandyopadhyay, I.; Lee, H. M.; Tarakeshwar, P.; Kim, K. S. *Theor. Chem. Acc.* **2006**, *115*, 127.
- (2) Singh, N. J.; Lee, H. M.; Hwang, I.-C.; Kim, K. S. *Supramol. Chem.* **2007**, *19*, 321.
- (3) (a) Re, S.; Osamura, Y.; Suzuki, Y.; Schaefer, H. F., III *J. Chem. Phys.* **1998**, *109*, 973. (b) Lee, C.; Sosa, C.; Novoa, J. J. *J. Chem. Phys.* **1995**, *103*, 4360. (c) Lee, C.; Sosa, C.; Planas, M.; Novoa, J. J. *J. Chem. Phys.* **1996**, *104*, 7081. (d) Planas, M.; Lee, C.; Novoa, J. J. *J. Phys. Chem.* **1996**, *100*, 16495. (e) Olleta, A. C.; Lee, H. M.; Kim, K. S. *J. Chem. Phys.* **2007**, *126*, 14311. (f) Olleta, A. C.; Lee, H. M.; Kim, K. S. *J. Chem. Phys.* **2006**, *124*, 024321. (g) Jungwirth, P. *J. Phys. Chem. A* **2000**, *104*, 145. (h) Cabaleiro-Lago, E. M.; Hermida-Ramon, J. M.; Rodriguez-Otero, J. *Chem. Phys.* **2002**, *177*, 3160.
- (4) (a) Odde, S.; Pak, C.; Lee, H. M.; Kim, K. S.; Mhin, B. J. *J. Chem. Phys.* **2004**, *121*, 204. (b) Kumar, A.; Park, M.; Huh, J. Y.; Lee, H. M.; Kim, K. S. *J. Phys. Chem. A* **2006**, *110*, 12484. (c) Odde, S.; Mhin, B. J.; Lee, K. H.; Lee, H. M.; Tarakeshwar, P.; Kim, K. S. *J. Phys. Chem. A* **2006**, *110*, 7918. (d) Singh, N. J.; Yi, H.-B.; Min, S. K.; Park, M.; Kim, K. S. *J. Phys. Chem. B* **2006**, *110*, 3808.
- (5) (a) Robertson, W. H.; Johnson, M. A. *Science* **2002**, *298*, 4. (b) Odde, S.; Mhin, B. J.; Lee, S.; Lee, H. M.; Kim, K. S. *J. Chem. Phys.* **2004**, *120*, 9524.
- (6) Perrin, D. B. *Ionization Constants of Inorganic Acids and Bases in Aqueous Solution*, 2nd ed.; Pergamon: Oxford, 1982.
- (7) (a) Dyke, T. R.; Herbine, P. *J. Chem. Phys.* **1985**, *83*, 3768. (b) Herbine, P.; Hu, T. A.; Johnson, G.; Dyke, T. R. *J. J. Chem. Phys.* **1990**, *93*, 5485. (c) Stockman, P. A.; Burngarner, R. E.; Suzuki, S.; Blake, G. A. *J. Chem. Phys.* **1992**, *96*, 2496.
- (8) (a) Sadlej, J.; Moszynski, R.; Dobrowolski, C. Cz.; Mazurk, A. P. *J. Phys. Chem. A* **1999**, *103*, 8528. (b) Astrand, P. O.; Karlstrom, G.; Engdahl, A.; Nelander, B. *J. Chem. Phys.* **1995**, *102*, 3534.
- (9) Donaldson, D. J. *J. Phys. Chem. A* **1999**, *103*, 62.
- (10) (a) Lee, C.; Fitzgerald, G.; Planas, M.; Novoa, J. J. *J. Phys. Chem. B* **1996**, *100*, 7398. (b) Bacelo, D. E. *J. Phys. Chem. A* **2002**, *106*, 11190.
- (11) (a) Liu, K.; Brown, M. G.; Saykally, R. J. *Science* **1996**, *271*, 62. (b) Gruenloh, C. J.; Carney, J. R.; Arrington, C. A.; Zwier, T. S.; Fredericks, S. Y.; Jordan, K. D. *Science* **1997**, *276*, 1678. (c) Buck, U.; Huisken, F. *Chem. Rev.* **2000**, *100*, 3863. (d) Nauta, K.; Miller, R. E. *Science* **2000**, *287*, 293.
- (12) (a) Buck, U.; Ettischer, I.; Melzer, M.; Buch, V.; Sadlej, J. *J. Phys. Rev. Lett.* **1998**, *80*, 2578. (b) Sadlej, J.; Buch, V.; Kazimirski, J. K.; Buck, U. *J. Phys. Chem.* **1999**, *103*, 4933.
- (13) (a) Mhin, B.-J.; Kim, H. S.; Kim, H. S.; Yoon, J. W.; Kim, K. S. *Chem. Phys. Lett.* **1991**, *176*, 41. (b) Kim, K. S.; Mhin, B. J.; Choi, U. S.; Lee, K. *J. Chem. Phys.* **1992**, *97*, 6649. (c) Mhin, B. J.; Kim, J.; Lee, S.; Lee, J. Y.; Kim, K. S. *J. Chem. Phys.* **1994**, *100*, 4484.
- (14) Franken, A.; Jalai, M.; Dykstra, C. E. *Chem. Phys. Lett.* **1992**, *198*, 59.
- (15) (a) Mo, O.; Yanez, M.; Elguero, J. *J. Chem. Phys.* **1992**, *97*, 6628. (b) Wales, D. J.; Ohmine, I. *J. Chem. Phys.* **1993**, *98*, 7245. (c) Schutz, M.; Klopper, W.; Luthi, H.-P.; Leutwyler, S. *J. Chem. Phys.* **1995**, *103*, 6114.
- (16) (a) Xantheas, S. S.; Dunning, T. H., Jr *J. Chem. Phys.* **1993**, *98*, 8037. (b) Hodges, M. P.; Stone, A. J.; Xantheas, S. S. *J. Phys. Chem. A* **1997**, *101*, 9163. (c) Fanourakis, G. S.; Apra, E.; Xantheas, S. S. *J. Chem. Phys.* **2004**, *121*, 2655.
- (17) (a) Tsai, C. J.; Jordan, K. D. *Chem. Phys. Lett.* **1993**, *213*, 181. (b) Pedulla, J. M.; Vila, F.; Jordan, K. D. *J. Chem. Phys.* **1996**, *105*, 11091.
- (18) (a) Kim, J.; Kim, K. S. *J. Chem. Phys.* **1998**, *109*, 5886. (b) Kim, J.; Majumdar, D.; Lee, H. M.; Kim, K. S. *J. Chem. Phys.* **1999**, *110*, 9128. (c) Lee, H. M.; Suh, S. B.; Lee, J. Y.; Tarakeshwar, P.; Kim, K. S. *J. Chem. Phys.* **2000**, *112*, 9759. (d) Lee, H. M.; Suh, S. B.; Kim, K. S. *J. Chem. Phys.* **2001**, *114*, 10749.
- (19) (a) Feyereisen, M. W.; Feller, D.; Dixon, D. A. *J. Phys. Chem.* **1996**, *100*, 1993. (b) Gregory, J. K.; Clary, D. C. *J. Phys. Chem.* **1996**, *100*, 18014. (c) Khan, A. *J. Chem. Phys.* **1997**, *106*, 5537. (d) Kryachki, E. S. *Chem. Phys. Lett.* **1997**, *272*, 132.
- (20) (a) Estrin, D. A.; Paglieri, L.; Corongiu, G.; Clementi, E. *J. Phys. Chem.* **1996**, *100*, 8701. (b) Kim, K. S.; Dupuis, M.; Lie, G. C.; Clementi, E. *Chem. Phys. Lett.* **1986**, *131*, 451. (c) van Duijneveldt-van de Rijdt, J. G. C. M.; van Duijneveldt, F. B. *Chem. Phys. Lett.* **1995**, *23*, 560.
- (21) (a) Lenz, A.; Ojamae, L. *J. Phys. Chem. A* **2006**, *110*, 13388. (b) Ojamae, L.; Shavitt, I.; Singer, S. J. *J. Chem. Phys.* **1998**, *109*, 5547.
- (22) Fowler, J. E., III *J. Am. Chem. Soc.* **1995**, *117*, 446.
- (23) (a) Lee, H. M.; Tarakeshwar, P.; Park, J. W.; Kolaski, M. R.; Yoon, Y. J.; Yi, H.-B.; Kim, W. Y.; Kim, K. S. *J. Phys. Chem. A* **2004**, *108*, 2949. (b) Kim, J.; Lee, S.; Cho, S. J.; Mhin, B. J.; Kim, K. S. *J. Chem. Phys.* **1995**, *102*, 839. (c) Kim, K. S.; Vercauteren, D. P.; Welti, M.; Chin, S.; Clementi, E. *Biophys. J.* **1985**, *47*, 327. (d) Kołaski, M.; Lee, H. M.; Pak, C.; Kim, K. S. *J. Am. Chem. Soc.* **2008**, *130*, 103. (e) Lee, H. M.; Kim, D.; Singh, N. J.; Kolaski, M.; Kim, K. S. *J. Chem. Phys.* **2007**, *127*, 164311.
- (24) (a) Shin, I.; Park, M.; Min, S. K.; Lee, E. C.; Suh, S. B.; Kim, K. S. *J. Chem. Phys.* **2006**, *125*, 234305. (b) Singh, N. J.; Park, M.; Min, S. K.; Suh, S. B.; Kim, K. S. *Angew. Chem., Int. Ed.* **2006**, *45*, 3795; *Angew. Chem.* **2006**, *118*, 3879.
- (25) Frauenheim, T.; Seifert, G.; Elstner, M.; Niehaus, T.; Köhler, C.; Amkreutz, M.; Sternberg, M.; Hajnal, Z.; Carlo, A. D.; Suhai, S. *J. Phys.: Condens. Matter* **2002**, *14*, 3049.
- (26) Weigend, F.; Haser, M. *Theor. Chem. Acc.* **1997**, *97*, 331.
- (27) (a) Min, S. K.; Lee, E. C.; Lee, H. M.; Kim, D. Y.; Kim, D.; Kim, K. S. *J. Comput. Chem.* **2008**, *29*, 1208. (b) Xantheas, S. S. *J. Chem. Phys.* **1996**, *104*, 8821.
- (28) Frisch, M. J.; Trucks, G. W.; Schlegel, H. B.; Scuseria, G. E.; Robb, M. A.; Cheeseman, J. R.; Montgomery, J. A., Jr.; Vreven, T.; Kudin, K. N.; Burant, J. C.; Millam, J. M.; Iyengar, S. S.; Tomasi, J.; Barone, V.; Mennucci, B.; Cossi, M.; Scalmani, G.; Rega, N.; Petersson, G. A.; Nakatsuji, H.; Hada, M.; Ehara, M.; Toyota, K.; Fukuda, R.; Hasegawa, J.; Ishida, M.; Nakajima, T.; Honda, Y.; Kitao, O.; Nakai, H.; Klene, M.; Li, X.; Knox, J. E.; Hratchian, H. P.; Cross, J. B.; Bakken, V.; Adamo, C.; Jaramillo, J.; Gomperts, R.; Stratmann, R. E.; Yazyev, O.; Austin, A. J.; Cammi, R.; Pomelli, C.; Ochterski, J. W.; Ayala, P. Y.; Morokuma, K.; Voth, G. A.; Salvador, P.; Dannenberg, J. J.; Zakrzewski, V. G.; Dapprich, S.; Daniels, A. D.; Strain, M. C.; Farkas, O.; Malick, D. K.; Rabuck, A. D.; Raghavachari, K.; Foresman, J. B.; Ortiz, J. V.; Cui, Q.; Baboul, A. G.; Clifford, S.; Cioslowski, J.; Stefanov, B. B.; Liu, G.; Liashenko, A.; Piskorz, P.; Komaromi, I.; Martin, R. L.; Fox, D. J.; Keith, T.; Al-Laham, M. A.; Peng, C. Y.; Nanayakkara, A.; Challacombe, M.; Gill, P. M. W.; Johnson, B.; Chen, W.; Wong, M. W.; Gonzalez, C.; Pople, J. A. *Gaussian 03*, revision C.02; Gaussian, Inc.: Wallingford, CT, 2004.
- (29) Ahlrichs, R.; Bar, M.; Haser, M.; Horn, H.; Kohl, C. *Chem. Phys. Lett.* **1989**, *162*, 165.
- (30) Lee, S. J.; Chung, H. Y.; Kim, K. S. *Bull. Korean Chem. Soc.* **2004**, *25*, 1061.

- (31) (a) Wei, D.; Salahub, D. R. *J. Chem. Phys.* **1997**, *106*, 6086. (b) Park, M.; Shin, I.; Singh, N. J.; Kim, K. S. *J. Phys. Chem. A* **2007**, *111*, 10692. (c) Mella, M.; Clary, D. C. *J. Chem. Phys.* **2003**, *119*, 10048. (d) McCoy, A. B.; Huang, X.; Carter, S.; Landeweer, M. Y.; Bowman, J. M. *J. Chem. Phys.* **2005**, *122*, 061101.
- (32) (a) Lee, H. M.; Tarakeshwar, P.; Kim, K. S. *J. Chem. Phys.* **2004**, *121*, 4657. (b) Robertson, W. H.; Diken, E. G.; Price, E. A.; Shin, J.-W.; Johnson, M. A. *Science* **2003**, *299*, 1367.
- (33) Kim, K. S.; Tarakeshwar, P.; Lee, J. Y. *Chem. Rev.* **2000**, *100*, 4145.
- (34) (a) Lisy, J. M. *Int. Rev. Phys. Chem.* **1997**, *16*, 267. (b) Brutschy, B. *Chem. Rev.* **2000**, *100*, 3891. (c) Lisy, J. M. *J. Chem. Phys.* **2006**, *125*, 132302. (d) Diken, E. G.; Hammer, N. I.; Johnson, M. A. *J. Chem. Phys.* **2005**, *123*, 164309.
- (35) (a) Benedict, W. S.; Gailar, N.; Plyler, E. K. *J. Chem. Phys.* **1956**, *24*, 1139. (b) Fraley, P. E.; Rao, K. N. *J. Mol. Spectrosc.* **1969**, *29*, 348.

JP801678R